Physiological Characterization of Pressure-Strain Loops Indices as Non-Invasive Surrogates for Ventriculo-Arterial Coupling: A Proof-of-Concept Study

Lígia Mendes

s-lilomendes@ucp.pt

Católica Medical School

João Colaço

Hospital da Luz Lisboa

José Ferreira Santos

Católica Medical School

João Pereira

Centro de Investigação Interdisciplinar em Saúde

Ana Teresa Timóteo

Unidade Local De Saúde de São José, Hospital de Santa Marta

Article

Keywords: Pressure–strain loop, Ventriculo-arterial coupling, Speckle-tracking echocardiography, Myocardial work, Myocardial mechanics, Non-invasive hemodynamics

Posted Date: March 30th, 2026

DOI: https://doi.org/10.21203/rs.3.rs-9172437/v1

Additional Declarations: No competing interests reported.

Version of Record: A version of this preprint was published at Scientific Reports on April 30th, 2026. See the published version at https://doi.org/10.1038/s41598-026-51048-2.

Abstract

Pressure–strain loop (PSL) analysis integrates myocardial deformation with estimated left-ventricular pressure and may provide a non-invasive approach to assess ventriculo-arterial coupling. However, its physiological behavior under controlled hemodynamic stress has not been systematically evaluated in humans. In this prospective physiologic study, healthy volunteers underwent standardized hemodynamic maneuvers. One cohort performed semi-supine exercise (contractility-dominant), while a second cohort underwent isometric handgrip followed by modified passive leg raising (afterload- and preload-modulating maneuvers). Left-ventricular PSL indices were derived from speckle-tracking echocardiography combined with brachial pressure calibration. Five pre-specified PSL indices reflecting afterload (arterial elastance, end-systolic pressure), contractility (systolic strain rate, peak systolic strain), and myocardial work (global work index) were defined as co-primary endpoints. Within-subject changes were analyzed using paired tests with Holm–Bonferroni correction. Exercise produced large increases in contractility-sensitive indices (Cohen's dz 0.88–1.29, all adjusted $p < 0.001$), while pressure indices rose selectively with handgrip and modified passive leg raising (Cohen's dz 0.77–1.21, adjusted $p \leq 0.001$). These findings demonstrate that PSL analysis detects physiologically meaningful hemodynamic responses in humans and provides non-invasive indices consistent with established ventricular–arterial coupling dynamics.

Introduction

The interaction between the left ventricle (LV) and the arterial system, termed ventriculo-arterial (VA) coupling, is a fundamental determinant of cardiovascular performance. Based in Otto Frank's seminal pressure–volume (PV) framework, VA coupling describes how the heart's contractile properties adapt to the load imposed by the arterial tree to preserve efficiency and optimize stroke work [1–3]. Quantifying this interaction provides an integrated measure of cardiac energetics and mechanical performance, both under physiological conditions and in diseases [4–6].

The invasive PV loop remains the reference standard for assessing LV mechanics and VA coupling, enabling derivation of key indices such as end-systolic elastance ventricular (Ees) and effective arterial elastance (Ea). However, this technique requires conductance catheterization, meticulous calibration, and specialized expertise, rendering it impractical for routine use or serial assessments [7,8].

To overcome these limitations, Russell et al. introduced the left ventricular pressure–strain loop (LV-PSL) analysis, which combines an estimated LV pressure curve (scaled from brachial cuff pressure and echocardiographic valve timing), with myocardial strain obtained by speckle-tracking echocardiography [9]. The enclosed loop area represents the Global Work Index (GWI), a measure of myocardial work expressed in mmHg*%. This non-invasive index correlates strongly with myocardial oxygen consumption and metabolic demand, providing a physiologically meaningful surrogate of regional cardiac work. Further validation studies have demonstrated that PSL-derived indices, such as Global Constructive Work and GWI, correspond closely with invasively measured parameters, even when absolute pressure

estimates vary modestly [10]. Of particular interest is the derivation of a pressure-strain domain analogue of effective arterial elastance (Ea_{PSL} = ESP/peak systolic strain), which extends the PSL framework beyond myocardial work to directly index ventriculo-arterial coupling, a construct previously accessible only through invasive conductance catheterisation. Despite this promise, the physiological responsiveness of the full LV-PSL index panel, including this novel coupling surrogate, across standardised hemodynamic stressors remains incompletely characterised. The present proof-of-concept study aims to address this gap by quantifying the response of non-invasive LV-PSL indices to standardised hemodynamic stressors designed to elicit contractility-dominant (exercise), afterload-dominant (isometric handgrip), and combined preload–afterload (modified passive leg raising, PRL) responses, hypothesising that these metrics will reflect predictable haemodynamic shifts consistent with established pressure-volume physiology [6,7].

Results

Participant Characteristics

Recruitment continued until achieving 30 high-quality acquisitions per intervention: 56 volunteers were screened for exercise (31 analyzable) and 47 for Handgrip/ modified PRL (30 analyzable). Importantly, the baseline demographic and hemodynamic characteristics of the participants included in the final analyses were not different from those of the total enrolled cohorts, indicating no significant selection bias (**Supplementary Table S2)**.

Among included volunteers, women comprised 65% of the exercise cohort versus 47% of those undergoing bedside maneuvers. Mean age was similar between groups (42 ± 8 vs. 43 ± 8 years). Resting brachial blood pressure was comparable (systolic 122 ± 15 vs. 121 ± 20 mmHg; diastolic 72 ± 8 vs. 69 ± 9 mmHg), though BMI was higher in the exercise cohort (29.0 ± 4.7 vs. 25.1 ± 3.2 kg/m²).

Both the exercise and the maneuvers group demonstrated echocardiographic parameters consistent with healthy cardiovascular function. Baseline GWI was 1,413 ± 287 mmHg% in the exercise group and 1,684 ± 276 mmHg% in the maneuvers group; GWE (global work efficiency) was 90 ± 4% and 95 ± 2%, respectively, consistent with published reference ranges [11,12]. Systolic strain rate, and early diastolic strain rate were all within expected physiological limits, confirming an appropriate healthy baseline before intervention. The baseline hemodynamic and echocardiographic characteristics of the 61 participants included in the final analyses are presented in Table 1.

Table 1
Baseline hemodynamic and echocardiographic characteristics

Basal Characteristic	**Group 1 Exercise** **N = 31**[1]	**Group 2 Manoeuvres** **N = 30**[1]
Estimated End Diastolic Pressure (mmHg)	8.84 ± 1.06	8.61 ± 0.67
End systolic pressure estimate (mmHg)	109 ± 13	106 ± 8
GWE (%)	90 ± 4	95 ± 2
GWI (mmHg*%)	1,413 ± 287	1,684 ± 276
GCW (mmHg*%)	1,780 ± 346	2,015 ± 312
GWW (mmHg*%)	179 ± 107	99 ± 43
End-diastolic fiber stress (%)	0.043 ± 0.005	0.045 ± 0.006
Peak systolic strain (%)	14.93 ± 2.01	18.75 ± 2.67
Systolic strain rate (s^{-1})	0.72 ± 0.12	0.82 ± 0.10
Early-diastolic strain rate (s^{-1})	0.41 ± 0.20	0.68 ± 0.36
Systolic duration (ms)	279 ± 32	279 ± 28
IVRT (ms)	101 ± 4	100 ± 8
Filling Time (ms)	464 ± 141	572 ± 149
Total diastolic time (ms)	565 ± 142	672 ± 147
Systolic time proportion	0.34 ± 0.05	0.30 ± 0.04
IVRT proportion	0.123 ± 0.020	0.109 ± 0.022
Filling time proportion	0.54 ± 0.06	0.59 ± 0.05
Ea (mmHg/%)	7.49 ± 1.30	5.89 ± 0.98
[1] Mean ± SD		

Abbreviations: Ea (arterial elastance=end systolic pressure/peak systolic strain); Filling time proportion (fraction [filling time/cycle length]); GCW (global constructive work); GWE (global work efficiency); GWI (global work index); GWW (global wasted work); IVRT (isovolumic relaxation time); IVRT proportion (fraction [IVRT time/cycle length]); Systolic time proportion (fraction [systole time/cycle length]).

Baseline Spearman correlations among the five co-primary endpoints ranged from negligible to moderate (|r| = 0.005–0.781; **Supplementary Table S3**); the highest association was between Ea and

peak systolic strain (r = − 0.849), consistent with their formula relationship and the expected physiological antagonism between afterload and myocardial deformation.

Co-Primary Endpoints

Across the three interventions, within-subject changes followed the pre-specified physiological directions, and several reached significance after Holm–Bonferroni correction (Fig. 1). Full change scores, effect sizes with 95% CI, and adjusted p-values are provided in **Supplementary Table S4.**

Exercise significantly increased all contractility-related parameters: systolic strain rate (SSR), GWI, peak systolic strain, and end-systolic pressure (all adjusted $p < 0.001$). Arterial elastance remained unchanged, indicating a contractility-dominant response (**Supplementary Table S5**).

In contrast, handgrip and PLR primarily increased afterload indices: both interventions significantly elevated end-systolic pressure and arterial elastance (adjusted $p \leq 0.001$), while effects on GWI, peak systolic strain, and systolic strain rate were small and not significant after multiplicity correction (**Supplementary Tables S6 and S7**).

Sensitivity Analyses of the Co-Primary Endpoints.

Only three outliers were identified across all 15 endpoint–intervention combinations. All nine combinations retaining significance after Holm-Bonferroni correction showed complete robustness across all sensitivity methods, with significance persisting after outlier removal, winsorization, permutation testing, and bootstrap confidence intervals excluding zero in all cases.

Two endpoint lost statistical significance following correction: PLR peak systolic strain (adjusted $p = 0.066$) and handgrip GWI (adjusted $p = 0.061$). However, both showed consistent directional effects across all sensitivity analyses, suggesting that the lack of significance after adjustment could reflect the conservative correction rather than the absence of physiological response (**Supplementary Table S8**).

Secondary Endpoints

Secondary endpoints were analyzed exploratorily without multiplicity correction; p-values are nominal and findings hypothesis-generating. Effect sizes guided interpretation across four domains: hemodynamics, myocardial work, loop morphology, and diastolic timing (Fig. 2; **Supplementary Table S9**).

Exercise produced the largest effects across domains, particularly for heart rate, systolic blood pressure, time to peak strain, global constructive work, and isovolumic relaxation time (IVRT) proportion, with reciprocal shortening of absolute diastolic filling times. Handgrip showed large effects primarily for heart rate and blood pressure, with diastolic timing changes secondary to rate acceleration. PLR effects

were predominantly limited to blood pressure increases, with minimal impact on myocardial work or temporal parameters.

Superimposed LV-PSL illustrates changes in ventriculo-arterial coupling across conditions, with morphological shifts consistent with those reported from invasive pressure–volume catheterization (Fig. 3).

Intra- and interobserver reliability

Intraclass correlation coefficients demonstrated good-to-excellent intra-observer reliability across all four assessed parameters (Ea, SSR, peak systolic strain, and GWI), with coefficients of variation ranging from 7.1% for peak systolic strain to 10.6% for GWI. Inter-observer reliability was good for Ea, SSR, and peak systolic strain, and moderate for GWI (**Supplementary Figure S1**). Bland–Altman plots showed small mean differences without statistically significant bias ($p \geq 0.25$, for mean bias) and no evidence of proportional bias ($p \geq 0.18$). Plots, together with the full numerical reproducibility metrics, are presented in the **Supplementary Figures S2 and S3.**

Discussion

In this proof-of-concept study, we evaluated LV-PSL as a non-invasive framework consistent with established pressure–volume loop physiology for assessing ventricular–arterial interactions. Using only standard apical 2D echocardiographic views and brachial cuff pressure, LV-PSL-derived indices were able to track within-subject responses to isometric handgrip, PLR and semi-supine exercise. Across primary interventions, the direction and magnitude of changes in afterload, deformation, and myocardial work were broadly consistent with *a priori* hypotheses derived from invasive PV loops literature [13–16], supporting the physiological validity of LV-PSL-based metrics as non-invasive surrogates of VA coupling dynamics.

In contrast to conductance-catheter PV analysis, which remains the reference standard but is invasive and resource-intensive [7,17], the present protocol demonstrates that LV-PSL-based assessments can be implemented in a routine echocardiography setting.

The most coherent and robust pattern emerged during exercise. Four of five co-primary endpoints (systolic strain rate, peak systolic strain, end-systolic pressure, and GWI) exhibited large effect sizes (Cohen's dz 0.9–1.3) and remained significant after Holm–Bonferroni correction. Arterial elastance PSL-derived showed no significant change. The pattern of marked augmentation of contractility-sensitive strain indices and myocardial work without a corresponding rise in afterload, aligns with PV-based descriptions of dynamic exercise, in which enhanced inotropy and heart rate increase end-systolic ventricular elastance and stroke work while effective arterial load remains relatively stable [14,18].

Secondary endpoints analyses further refine this interpretation. Exercise produced large effect-size increases in heart rate, systolic blood pressure, and global constructive work, alongside a medium-to-large effect-size rise in early diastolic strain rate and marked shortening of time to peak strain. IVRT proportion showed a medium effect-size increase, while absolute filling time and total diastolic time decreased markedly; filling-time proportion and end-diastolic fiber stress showed negligible changes. Collectively, these findings indicate a contractility-dominant response with preserved or enhanced relaxation kinetics despite diastolic time compression, consistent with the expected prioritization of pump performance during dynamic exercise [18].

Both handgrip and PLR produced a pressure-dominant hemodynamic profile, with large increases in end-systolic pressure and Ea (Cohen's dz 0.8–1.2) and only small, non-significant changes in strain and work-based co-primary endpoints. For handgrip, this was the expected response to isometric afterload augmentation [6,7]. For PLR, the pressure-dominant pattern reflects the mixed preload–afterload effects of the modified positioning protocol, in which self-supported leg elevation with knee flexion likely raised peripheral resistance alongside venous return.

For handgrip, secondary endpoints confirmed a pressure-driven response: systolic blood pressure and heart rate increased markedly (both large effect sizes), diastolic pressure rose to a lesser extent, and global constructive work showed a moderate increase without a change in global work efficiency. End diastolic fiber stress and diastolic timing changes were small and explained by the heart rate acceleration. These findings are in agreement with previous reports that isometric handgrip acutely raises arterial load and blood pressure with only limited modification of intrinsic contractility in healthy individuals [19].

As described above, the modified PLR positioning produced a pressure-dominant hemodynamic profile. Systolic and diastolic blood pressure, end-systolic pressure, and Ea all increased substantially, while heart rate, deformation indices, and myocardial work parameters changed little. The absence of significant changes in peak strain, GWI, and GCW is consistent with afterload-mediated offset of any Frank–Starling–driven contractile augmentation, a pattern that contrasts with the stroke volume augmentation reported in classical passive leg raising protocols [20].

Beyond directionality, the robustness and reproducibility of pressure-strain loop metrics are critical if they are to be deployed for serial monitoring. Nine of fifteen intervention-endpoint combinations met the Holm–Bonferroni threshold. All significant findings remained stable across sensitivity analyses, including outlier removal, winsorization, permutation testing, and bootstrap confidence intervals, with 93% of intervention-endpoint pairs showing concordant results.

Measurement reliability was similarly encouraging. Intra-observer ICC values were in the good-to-excellent range for all four assessed parameters, while inter-observer agreement was good for Ea, SSR, and peak systolic strain, and moderate for GWI. Coefficients of variation ranged from 7% to 11%, and Bland–Altman analysis revealed no significant systematic or proportional bias. These metrics are

comparable to, or slightly better than, previously reported values for global longitudinal strain and myocardial work indices [21–23]. Importantly, the analysis relies on 2D speckle-tracking rather than 3D full-volume acquisitions, a practical advantage, as 2D imaging is faster and generally more robust in tachycardia, irregular rhythm, and dilated ventricles, where 3D datasets are often suboptimal [16,24].

Taken together, these data demonstrate that LV-PSL analysis can detect physiologically meaningful hemodynamic changes within individuals, with effect-size patterns that mirror established PV loop physiology under exercise and afterload stress. This has potential relevance for settings in which repeated invasive assessment is impractical, such as day-hospital interventions, serial monitoring in hemodynamically unstable patients, where robust non-invasive tools are needed [25]. At the research level, the pre-registered statistical framework with explicit multiplicity control and sensitivity analyses illustrates how LV-PSL methodology can be evaluated with appropriate rigor. Whether this approach translates to populations with hypertension, cardiomyopathies, or heart failure, where myocardial work indices have shown diagnostic and prognostic value, requires characterization in disease-specific cohorts [26].

Several limitations merit consideration. First, the primary cohort consisted of relatively young, healthy volunteers; generalizability to patients with advanced cardiovascular disease remains to be established. Second, the PLR maneuver used self-supported leg elevation with knee flexion rather than fully operator-mediated passive elevation, a departure from standardized technique that likely introduced afterload augmentation alongside venous return, limiting comparability with classical PLR protocols. Third, LV pressure waveforms were estimated by scaling a reference curve to brachial cuff pressure, an approach validated at rest but subject to greater uncertainty during exercise, when the morphology of the pressure waveform and the ratio of end-systolic to peak systolic pressure may deviate from resting assumptions. In the present study, brachial pressure was measured with the arm supported on a dedicated armrest during semi-supine cycling, minimising motion artefact; nonetheless, end-systolic pressure was estimated as 0.9 × brachial systolic pressure, a widely used approximation whose accuracy under haemodynamic stress warrants further validation against simultaneous invasive measurements. Furthermore, analyses were performed on a single commercial platform (EchoPAC, GE Healthcare); inter-vendor agreement for myocardial work indices is imperfect and results may not be directly comparable across software platforms. Finally, direct invasive pressure-volume measurements were not obtained simultaneously, so physiological characterisation relied on directional concordance with pre-specified hypotheses derived from established PV loop physiology rather than individual invasive validation.

In summary, this proof-of-concept study demonstrates that non-invasively derived pressure-strain loop indices are physiologically responsive to standardized hemodynamic interventions, with directional changes consistent with established pressure-volume physiology. The method captured the expected dominance of contractile reserve during exercise, demonstrated sensitivity to afterload changes during handgrip and modified PRL, and showed good-to-excellent intra- and inter-observer reliability. These findings provide a physiological foundation for further characterization of pressure-strain loop analysis

in clinical populations, with potential applications in serial hemodynamic monitoring and individualized therapeutic guidance.

Methods

Study design and participants

This was a prospective, within-subject, repeated-measures study in healthy adult volunteers. Exclusion criteria included hypertension, diabetes mellitus, dyslipidemia, current smoking, pregnancy, significant systemic illness, use of cardioactive medications (agents affecting heart rate, contractility, or vascular tone), and baseline echocardiographic abnormalities suggestive of structural heart disease.

Participants were allocated to one of two standardized intervention protocols designed to elicit predominantly domain-specific hemodynamic perturbations. Group 1 underwent semi-supine isotonic exercise (contractility-dominant). Group 2 performed isometric handgrip (predominantly afterload-increasing) followed by modified passive leg raising (PLR; preload augmentation with concurrent afterload change). PLR was performed with the legs supported on a platform in a tabletop position with flexed knees. In Group 2, a 5-minute recovery period was maintained between maneuvers.

All interventions were conducted in a controlled laboratory setting with contemporaneous brachial blood pressure acquisition. Semi-supine exercise was performed on a dedicated semi-supine cycle ergometer (Ergoline). Resistance was applied incrementally until a prespecified target of > 25 Watts and a heart rate of approximately 100 beats/min was reached, at which echocardiographic imaging was acquired. The 100 beats/min target was selected to ensure a physiologically meaningful haemodynamic perturbation while maintaining a frames-per-cardiac-cycle ratio adequate for reliable speckle-tracking analysis. Conventional 2D echocardiography at 50–70 fps provides approximately 30–40 frames per cardiac cycle at this heart rate, which is within the validated range for accurate deformation measurement [27]. Echocardiographic imaging was obtained at physiological steady state during handgrip, within the established post-PLR response window, and at the prespecified exercise target as described above.

As prespecified, analyses were restricted to participants with paired baseline and intervention acquisitions of adequate-to-optimal image quality for deformation (speckle-tracking) analysis. Enrollment was concluded once at least 30 valid paired acquisitions were obtained for each protocol.

Echocardiographic acquisition and PSL construction

Transthoracic echocardiography was obtained in apical two-, three-, and four-chamber views and analyzed offline in EchoPAC v204 (GE Healthcare®). Global longitudinal strain (GLS) was derived using speckle-tracking according to the methodology of the contemporary consensus [23]. A left-ventricular pressure waveform was estimated by scaling a reference curve to brachial systolic/diastolic pressures and aligning it to mitral and aortic valve timing. LV-PSL-derived indices included myocardial work

parameters (global work index (GWI), global constructive work (GCW), global wasted work (GWW), and global work efficiency (GWE)) and strain-based measures (peak systolic strain, systolic strain rate (SSR), end-diastolic fibre stress, and early diastolic strain rate), as well as filling time, diastolic time, and ratios [21–23,28].

The effective arterial elastance surrogate (Ea, mmHg/%) was derived analogously to pressure-volume loop methodology, where Ea = end-systolic pressure / stroke volume. Ea was calculated as the ratio of estimated end-systolic pressure (ESPest) to peak systolic strain, the functional analogue of stroke volume in the pressure-strain domain. In healthy adults, post-ejection shortening is negligible, such that peak systolic strain approximates strain range (the excursion from mitral to aortic valve closure), justifying this simplified expression. End-systolic pressure was estimated as 0.9 × brachial systolic blood pressure. This parameter represents the slope of the line from the origin to the end-systolic point in pressure–strain space and serves as a non-invasive index of afterload (see Fig. 3).

Endpoints

Five co-primary endpoints were pre-specified to capture distinct hemodynamic properties: Ea and end-systolic pressure (ESP), afterload; systolic strain rate (SSR) and peak systolic strain, contractility; and GWI, work/energetics. To assess the robustness of findings, sensitivity analyses were performed on all primary endpoints across interventions.

Secondary endpoints comprised qualitative loop-morphology assessment, directional and shape changes of LV-PSL pre- versus post-intervention, obtained by superimposing paired loops, and were interpreted against established pressure–volume behavior. Additional secondary measures included myocardial-work components (constructive/wasted work and global work efficiency) and ancillary timing indices.

Expected physiological directions (a priori)

Directional hypotheses for each endpoint under each intervention were defined *a priori* based on invasive PV loop data (**Supplementary Table S1**). Handgrip, as an afterload-augmenting maneuver, was expected to increase estimated end-systolic pressure and the Ea surrogate, with minimal or modest reductions in peak systolic strain. Exercise was hypothesized to increase systolic strain rate, augment peak systolic strain, and raise myocardial work indices, consistent with enhanced inotropy. PLR was anticipated to elicit a mixed hemodynamic profile rather than a purely preload-driven shift, with a preload-mediated increase in loop dimensions (GWI and loop width) accompanied by an afterload rise (Ea and end-systolic pressure) attributable to increased peripheral resistance in the flexed-leg position [15,13,14].

Data handling and reproducibility

EchoPAC exports (xml) were parsed using Python 3 to Pandas 2 data frames and exported to an Excel file. Custom Python utilities also generated superimposed LV-PSL to quantify loop-shape secondary

endpoints. Strain values are expressed in absolute numbers.

Statistical analysis

The Statistical Analysis Plan required at least 30 paired cases per intervention group; all power and precision calculations are detailed therein. Within-subject change scores (Δ = intervention − baseline) were tested per endpoint and intervention using the Shapiro–Wilk test for normality, followed by paired t-tests (normal distribution) or exact Wilcoxon signed-rank tests (non-normal distribution). Effect sizes were reported as Cohen's dz (parametric) or rank-biserial r (non-parametric) with 95% confidence intervals (CI), using standard thresholds: for Cohen's dz, negligible (< 0.2), small (0.2–0.5), medium (0.5–0.8), and large (> 0.8); for rank-biserial r, negligible (< 0.1), small (0.1–0.3), medium (0.3–0.5), and large (> 0.5). Multiplicity was controlled within intervention families using Holm–Bonferroni across the five co-primary endpoints (family-wise α = 0.05). Spearman correlation matrix was computed for the five co-primary endpoints at baseline to assess inter-endpoint relationships. Sensitivity analyses included outlier removal, Winsorization, permutation tests (1,999 sign-flips), and BCa (Bias-Corrected and accelerated) bootstrap CIs (1,999 resamples). Secondary endpoints were descriptive (p-values, effect sizes/CIs are only nominal). Reproducibility was assessed in a 15-participant subset using blinded duplicate reads with an ≥ 8-week washout to quantify intra- and inter-observer reliability (intraclass correlation coefficients with 95% CIs, ICC(3,1) for intra-observer and ICC(2,1) for inter-observer) [29] and agreement (Bland–Altman bias and limits with proportional-bias testing). Analyses were performed in R (RStudio version 2025.09.2 + 418).

Ethics and registration

The study complied with the principles of the Declaration of Helsinki[30]. All participants provided written informed consent before enrollment, and the protocol received approval from the Hospital da Luz Ethics Committee. The project is publicly registered on the Open Science Framework (OSF): https://doi.org/10.17605/OSF.IO/3QJGW.

Abbreviations

Ea – Arterial elastance (end-systolic pressure/peak systolic strain)

ESP – End-systolic pressure

GCW – Global constructive work

GLS – Global longitudinal strain

GWE – Global work efficiency

GWI – Global work index

GWW – Global wasted work

IVRT – Isovolumic relaxation time

LV – Left ventricle / left ventricular

LV-PSL – Left ventricular pressure–strain loop

OSF – Open Science Framework

PLR – Passive leg raising

PSL – Pressure–strain loop

PV – Pressure–volume

SBP – Systolic blood pressure

SSR – Systolic strain rate

VA – Ventriculo-arterial

Declarations

Acknowledgments:

The authors thank Sara Machado MD, João Patrício MD, Carla Costa MD, and Patrícia Patrício MD for their assistance with participant recruitment and data acquisition. This study was supported by GLSMED Learning Health, S.A. (grant code LH.INV.F2025007). The funders had no role in study design, data collection, analysis, decision to publish, or preparation of the manuscript.

Funding:

Funding was provided by GLSMED Learning Health, S.A. (grant code LH.INV.F2025007); the funders had no involvement in study design, data collection, analysis, or manuscript preparation.

Author contributions:

L.M. conceived and designed the study, acquired echocardiographic data, performed primary data analysis, and wrote the manuscript. J.C. developed the custom Python pipeline for superimposed pressure-strain loop generation. J.F.S. performed independent inter-observer variability measurements. J.P. supervised statistical methodology and validated the analytical approach. A.T.T. provided supervision and critical intellectual input throughout the project. All authors critically reviewed and approved the final manuscript.

Data availability: The data underlying this article will be made available by the corresponding author (Lígia Mendes M.D., s-lilomendes@ucp.pt) upon reasonable request.

Competing interests:

The authors declare no competing interests.

References

1. Kuhtz-Buschbeck, J. P., Drake-Holland, A., Noble, M. I. M., Lohff, B. & Schaefer, J. Rediscovery of Otto Frank's contribution to science. *J. Mol. Cell. Cardiol.* **119**, 96–103 (2018).
2. Suga, H. & CARDIAC ENERGETICS: FROM E_{MAX} TO PRESSURE–VOLUME AREA. *Clin. Exp. Pharmacol. Physiol.* **30**, 580–585 (2003).
3. Protti, I., Van Den Enden, A., Van Mieghem, N. M., Meuwese, C. L. & Meani, P. Looking Back, Going Forward: Understanding Cardiac Pathophysiology from Pressure–Volume Loops. *Biology* **13**, 55 (2024).
4. Sunagawa, K., Sagawa, K. & Maughan, W. L. Ventricular interaction with the loading system. *Ann. Biomed. Eng.* **12**, 163–189 (1984).
5. Starling, M. R. Left ventricular-arterial coupling relations in the normal human heart. *Am. Heart J.* **125**, 1659–1666 (1993).
6. Monge García, M. I. & Santos, A. Understanding ventriculo-arterial coupling. *Ann. Transl Med.* **8**, 795–795 (2020).
7. Bastos, M. B. et al. Invasive left ventricle pressure–volume analysis: overview and practical clinical implications. *Eur. Heart J.* **41**, 1286–1297 (2020).
8. Wo, N., Rajagopal, V., Cheung, M. M. H., Smolich, J. J. & Mynard, J. P. Assessment of single beat end-systolic elastance methods for quantifying ventricular contractility. *Heart Vessels*. **34**, 716–723 (2019).
9. Russell, K. et al. A novel clinical method for quantification of regional left ventricular pressure–strain loop area: a non-invasive index of myocardial work. *Eur. Heart J.* **33**, 724–733 (2012).
10. Hubert, A. et al. Estimation of myocardial work from pressure–strain loops analysis: an experimental evaluation. *Eur Heart J. - Cardiovasc Imaging*. **19**, 1372–1379 (2018).
11. Manganaro, R. et al. Echocardiographic reference ranges for normal non-invasive myocardial work indices: results from the EACVI NORRE study. *Eur Heart J. - Cardiovasc Imaging*. **20**, 582–590 (2019).
12. Truong, V. T. et al. Normal Ranges of Global Left Ventricular Myocardial Work Indices in Adults: A Meta-Analysis. *J. Am. Soc. Echocardiogr*. **35**, 369–377e8 (2022).
13. Penicka, M. et al. Heart Failure With Preserved Ejection Fraction in Outpatients With Unexplained Dyspnea. *J. Am. Coll. Cardiol.* **55**, 1701–1710 (2010).
14. Patterson, T. et al. Impact of coronary artery disease on contractile function and ventricular-arterial coupling during exercise: Simultaneous assessment of left-ventricular pressure–volume and coronary pressure and flow during cardiac catheterization. *Physiol Rep* **9**, (2021).

15. Rommel, K. P. et al. Extracellular Volume Fraction for Characterization of Patients With Heart Failure and Preserved Ejection Fraction. *J. Am. Coll. Cardiol.* **67**, 1815–1825 (2016).
16. Hammersboen, L. E. R. et al. Noninvasive Pressure-Volume Analysis by Three-Dimensional Echocardiography: A Novel Powerful Method for Evaluating Left Ventricular Function. *J. Am. Soc. Echocardiogr*. **38**, 946–958 (2025).
17. Chen, C. H. et al. Noninvasive single-beat determination of left ventricular end-systolic elastance in humans. *J. Am. Coll. Cardiol.* **38**, 2028–2034 (2001).
18. Chantler, P. D., Lakatta, E. G. & Najjar, S. S. Arterial-ventricular coupling: mechanistic insights into cardiovascular performance at rest and during exercise. *J. Appl. Physiol.* **105**, 1342–1351 (2008).
19. Jake Samuel, T. et al. Isometric handgrip echocardiography: A noninvasive stress test to assess left ventricular diastolic function. *Clin. Cardiol.* **40**, 1247–1255 (2017).
20. Sabatier, C., Monge, I., Maynar, J. & Ochagavia, A. Assessment of cardiovascular preload and response to volume expansion. *Med. Intensiva Engl. Ed.* **36**, 45–55 (2012).
21. Ilardi, F. et al. Myocardial Work by Echocardiography: Principles and Applications in Clinical Practice. *J. Clin. Med.* **10**, 4521 (2021).
22. Marzlin, N. et al. Myocardial Work in Echocardiography. *Circ Cardiovasc. Imaging* **16**, (2023).
23. Thomas, J. D. et al. Clinical Applications of Strain Echocardiography: A Clinical Consensus Statement From the American Society of Echocardiography Developed in Collaboration With the European Association of Cardiovascular Imaging of the European Society of Cardiology. *J. Am. Soc. Echocardiogr*. **38**, 985–1020 (2025).
24. Smiseth, O. A. et al. Myocardial Strain Imaging. *JACC Cardiovasc. Imaging*. **18**, 340–381 (2025).
25. Landra, F. et al. Pressure–strain loops unveil haemodynamics behind mechanical circulatory support systems. *ESC Heart Fail.* **10**, 2607–2620 (2023).
26. Chan, J. et al. A new approach to assess myocardial work by non-invasive left ventricular pressure–strain relations in hypertension and dilated cardiomyopathy. *Eur Heart J. - Cardiovasc Imaging*. **20**, 31–39 (2019).
27. Voigt, J. U. et al. Definitions for a common standard for 2D speckle tracking echocardiography: consensus document of the EACVI/ASE/Industry Task Force to standardize deformation imaging. *Eur Heart J. - Cardiovasc Imaging*. **16**, 1–11 (2015).
28. Abawi, D. et al. The non-invasive assessment of myocardial work by pressure-strain analysis: clinical applications. *Heart Fail. Rev.* **27**, 1261–1279 (2022).
29. Koo, T. K. & Li, M. Y. A Guideline of Selecting and Reporting Intraclass Correlation Coefficients for Reliability Research. *J. Chiropr. Med.* **15**, 155–163 (2016).
30. World Medical Association. World Medical Association Declaration of Helsinki: Ethical Principles for Medical Research Involving Human Participants. *JAMA* **333**, 71 (2025).

Figures

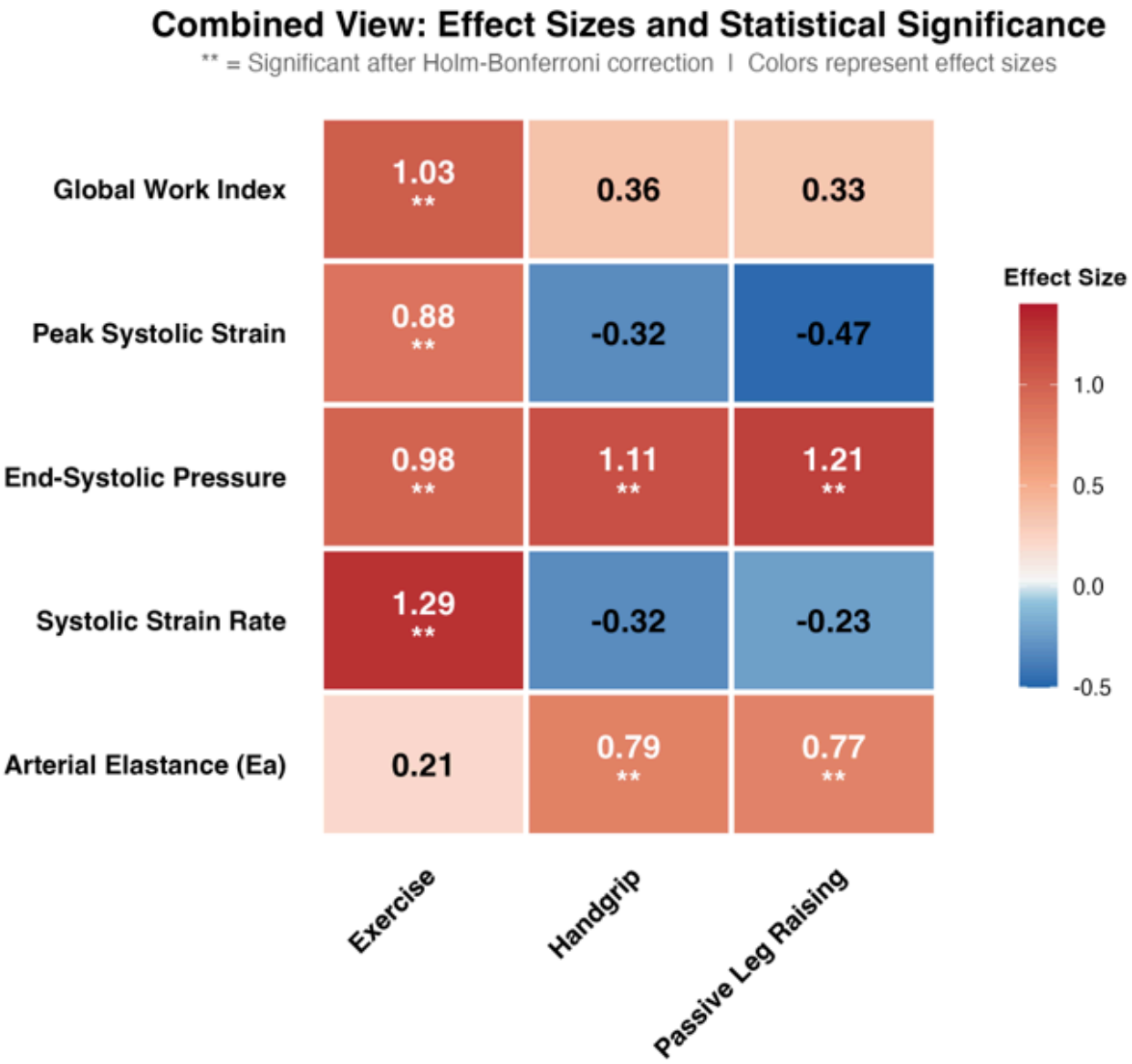

Figure 1

Effect Sizes and Statistical Significance for Five Co-Primary LV-PSL Endpoints Across Three Hemodynamic Interventions

Heatmap of effect sizes (Cohen's dz or rank-biserial r) for the five co-primary LV-PSL endpoints across three standardised hemodynamic interventions in 61 healthy volunteers. Cell colour indicates effect magnitude and direction (red = positive, blue = negative; colour intensity proportional to effect size). Double asterisks (**) denote significance after Holm–Bonferroni correction.

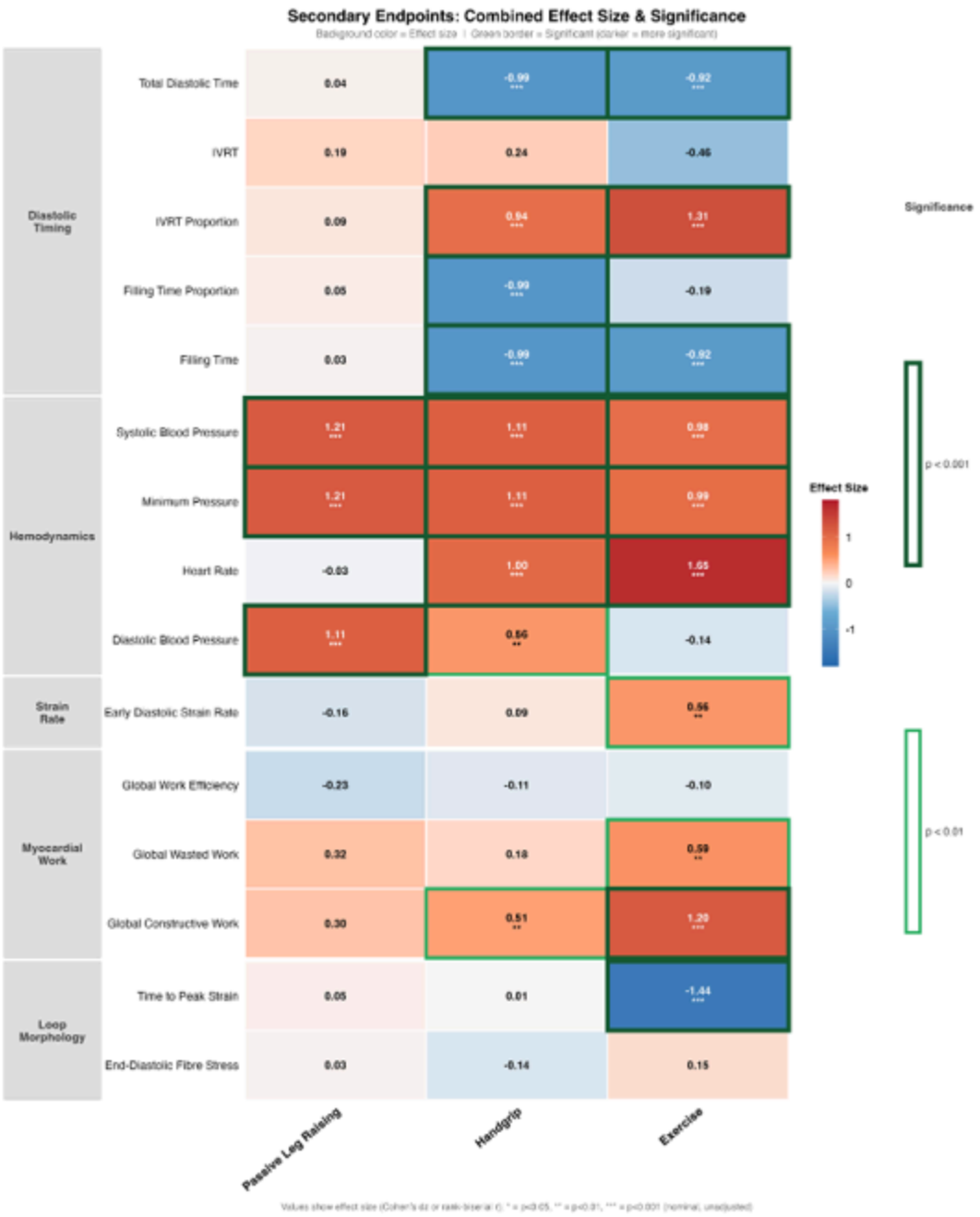

Figure 2

Exploratory Analysis of Secondary Endpoints: Combined Effect Size and Significance Heatmap

Heatmap visualization of exploratory secondary endpoint analyses across three hemodynamic interventions (Exercise, Handgrip, Passive Leg Raising). Cell background color represents Cohen's d effect size magnitude (red = positive effects, blue = negative effects; color intensity proportional to |dz|). Green borders indicate nominal statistical significance: darker borders denote p<0.001, brighter borders denote p<0.01(all unadjusted for multiple comparisons). Values within cells show effect sizes with significance markers (** p<0.01, *** p<0.001, nominal). Endpoints are organized by physiological category: Loop Morphology (temporal strain and fiber stress characteristics), Myocardial Work (global

work indices), Strain Rate (early diastolic relaxation), Hemodynamics (blood pressure and heart rate), and Diastolic Timing (IVRT and filling time proportions).

Abbreviations:IVRT (isovolumic relaxation time)

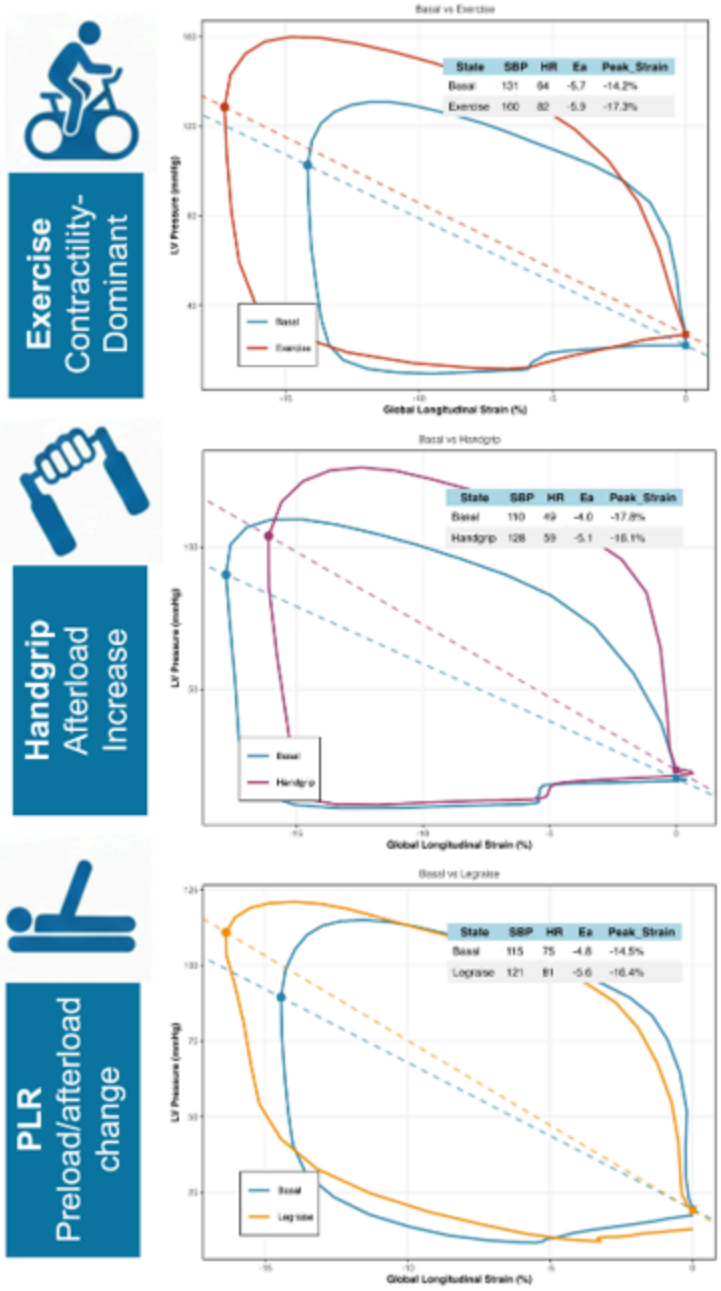

Figure 3

Pressure–Strain Loop Responses: Examples of Three Hemodynamic Interventions in a Healthy Volunteer

Representative pressure-strain loops at baseline (blue) and during intervention (red/purple/orange) for three distinct hemodynamic challenges. **Top panel:**Exercise (contractility-dominant response) demonstrates marked rightward and upward shift of the loop with increased area, reflecting enhanced myocardial work. **Middle panel:** Isometric handgrip (afterload increase) shows upward shift with minimal

horizontal displacement, indicating preserved contractility against increased vascular resistance. **Bottom panel:** Passive leg raising (preload/afterload changes) produces intermediate loop modifications with both horizontal and vertical components.

Dashed gray lines represent arterial Elastance (Ea) = ESP/ Peak systolic strain. Numerical values show systolic blood pressure (SBP), heart rate (HR), Ea (arterial elastance) and peak strain at baseline and during each intervention.

Abbreviations:ESP, end systolic pressure; LV, left ventricular; PLR, passive leg raising

Supplementary Files

This is a list of supplementary files associated with this preprint. Click to download.

- 0SuplementarymaterialScientificReports.pdf